JOURNAL OF THEORETICAL AND APPLIED MECHANICS
46, 2, pp. 291-303, Warsaw 2008

CRACK INITIATION AND GROWTH IN CIRCULAR SAW MADE OF TOOL STEEL

Ismail Ucun
Mehmet Colakoglu
Suleyman Tasgetiren

Department of Mechanics, Afyon Kocatepe University, Afyonkarahisar, Turkey
e-mail: iucun@aku.edu.tr; colakoglu@aku.edu.tr; tasgetir@aku.edu.tr

Fatigue of a circular saw made of tool steel and used in metal industry to cut, in particular, metal bars and pipes is investigated in this study. Due to having a small tooth root radius, the circular saw is much more likely to get crack damage at the tooth root region. Radial and tangential forces are also effective at this region for fatigue crack initiation. In high cutting speeds and feed rates of the circular saw, higher stress concentration occurs particularly at that region. To examine the fatigue and failure in the circular saw, specimens used in an experiment are prepared from a damaged circular saw are subjected to different mechanical tests. In the theoretical study, stress and fracture behaviour of the saw is determined by the finite element method. Results and causes of the failure are assessed and compared.

Key words: circular saw, failure analysis, crack, tool steel, finite element analysis

1. Introduction

A circular saw manufactured from tool steel is mostly used to cut profile cross-sectioned materials in metal industry. Feed rate and revolution speed (rpm) of a disk, type of a material being cut, etc., are important parameters for failure of the disk. Variable forces occur during the cutting process in the circular saw. When the disk starts to get dull, these forces get bigger (Andersson, 2001). As a result, undesired damage occurs at the tooth root region. The saw material is as important as the feed rate and cutting speed for wearing and damaging. Therefore, recent studies are especially focused on the development of better

materials and on manufacturing to protect saw, from damage (Nordström and Bergström, 2001).

Fukaura *et al.* (2004) investigated fatigue properties of two types of cold-work steels tempered at various temperatures. The S-N curves of steels were similar to those of most structural steels. The results showed that the sub-surface fatigue cracks initiation was dominant at lower alternating stresses. Yesildal *et al.* (2003) determined fatigue characteristics of the hot work tool steel X40CrMoV 51 at high temperatures. In the experiment, cylindrical specimens were used at the temperature range between 50-600°C. As a result, the fatigue limit of the material at room temperature was determined as 432 MPa, but it decreased to 383 MPa at 400°C and also stayed constant between 400-600°C.

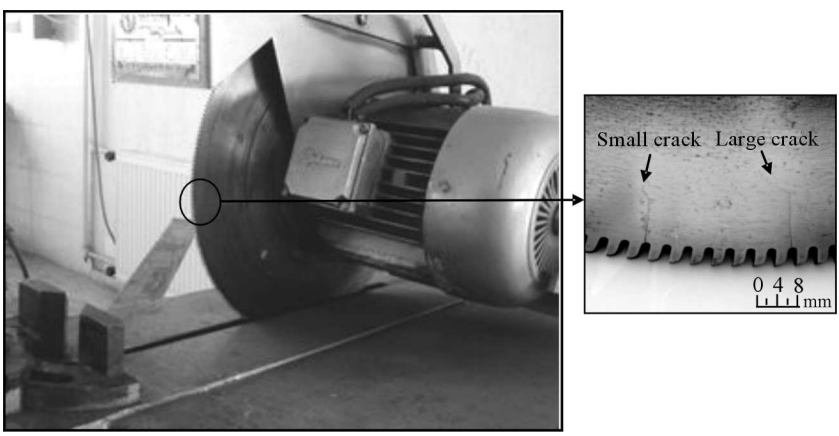

Fig. 1. A conventional cutting machine and a cracked circular saw

The aim of this study is to analyze the fatigue cracking of a circular saw encountered in a real application. In the analysis, stress and fracture behaviour is determined by using the finite element method. The classical cutting machine and circular saw used to cut profile cross-sectioned metals are shown in Fig. 1. Figure 1 also shows typical crack propagation in a circular saw. Dimensions of the saw and saw teeth are given in Fig. 2. Mechanical behaviour of the disk is investigated on specimens prepared from the tooth root region of the disk subjected to various mechanical tests. It is found that cracks under different loads grow at the tooth root regions of the circular saw since it has a small tooth root radius, which causes much higher stress concentration in this area.

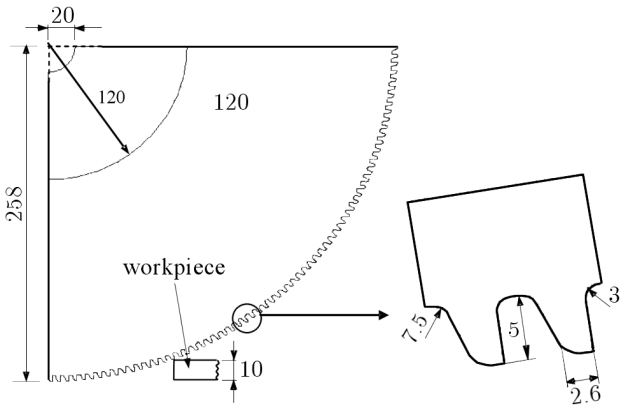

Fig. 2. Geometrical model of the circular saw with a work piece and geometry of the saw teeth

2. Experimental investigation

The specimens used in experiments consisting of mechanical tests, and chemical and metallographic analyses are prepared from a damaged circular saw. Three different mechanical tests, namely tensile, hardness and impact energy tests are carried out. The Instron and Psd 300/150-1 test machines are used for the tensile and impact energy tests, respectively. In addition, hardness measurements are carried out by a MetTest-HT type computer integrated hardness tester.

2.1. Chemical analysis

A sample extracted from the circular saw is applied to spectrometric chemical analysis, and the result of it is shown in Table 1.

Table 1. Chemical acomposition of the circular saw material [%wt]

C	Si	Mo	Mn	Ni	Cu	S	Al	V	Cr
0.586	0.202	0.066	0.420	0.032	0.060	0.028	0.011	0.183	0.585

Depending on the material composition in Table 1, it is estimated as the tool steel DIN 17210, which has 60 WCrV 7 (Heat Treaters Guide, 1995; Topbas, 1998). According to this Standard, Si and Cr must be kept between 0.55-0.7% and 0.9-1.2%, respectively, but it is found that Si is 0.202% and Cr is

0.585% in weight. As a result, lower Si element causes oxidation on the circular saw. In addition, lower Cr element in it decreases not only the transformation temperature and hardness but also significant amount of wear resistance.

2.2. Microstructure of the circular saw

When the microstructure of the circular saw material is analyzed, it is seen that the material is a tempered martensite. The microstructure of the circular saw is given in Fig. 3. Usually, a martensitic steel is tempered to increase ductility and toughness. The material of the circular saw is thought to be subjected to quenching at approximately 850°C which is followed by tempering at approximately 470°C (Heat Treaters Guide, 1995; ASM Speciality Handbook, 1996). Grain boundaries are not exactly seen in the microstructure analysis of the circular saw due to the tempering process.

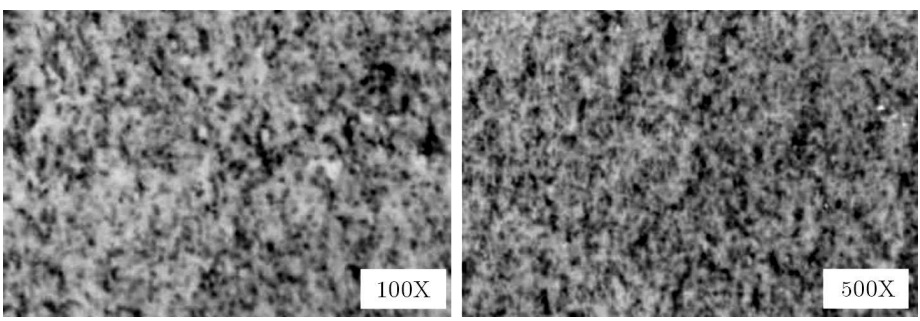

Fig. 3. Microstructure of the circular saw

2.3. Mechanical properties

The results of the mechanical tests are given in Table 2. Using the results of chemical analysis and mechanical tests, the material of the circular saw is estimated as a medium carbon alloy steel, DIN 17210, with a high tensile strength because of quenching and tempering. The hardness is measured as 43 HRC in the mid-part of the circular saw where no deformation occurs. On the other hand, severe heating that occurred during the cutting process decreases the hardness in tooth root regions, where it is measured as 39 HRC.

Table 2. Mechanical properties of the circular saw material

Elasticity modulus [GPa]	201
Poisson's ratio	0. 28
Yield strength [MPa]	640
Tensile strength [MPa]	1278
Total strain [%]	15.4
Hardness HRC	43
Impact energy with notch [J]	4.1

3. Analysis

3.1. Finite element modeling of the saw

The circular saw is modeled via Franc 2DL finite element software as shown in Fig. 4 (FRANC2D [8]). Because of symmetry, only one fourth of the saw geometry is drawn to simplify the problem. In addition, isoparametric triangular and quadrilateral elements are used together in the finite element model with 6967 nodes and 2938 elements in the solution domain. Also, boundary conditions are constructed around the hole circumference in the x and y directions. The material properties (modulus of elasticity and Poisson's ratio) of the saw (from Table 2) are entered into the program. To investigate the stress distribution, 2880 rpm, which is measured from the cutting machine and 10 mm constant depth of cut are applied to the model because this circular saw is usually used to cut bars having up to 10 mm thickness. Moreover, the forces are constructed in the normal and tangential directions, see Fig. 4. The maximum force occurs at the first contact point of the tooth. In the analysis, the maximum F_t and F_n are taken 2280 and 1845 N, respectively. These values are calculated using formulas from the theory of cutting (Akkurat, 1996; Bootroyd, 1989). The cutting forces are calculated depending on the depth of cut (10 mm), feed rate (631 mm/min), cutting velocity (2880 rpm) and material properties given in Table 2. The feed rate is measured for real cutting conditions.

3.2. Fracture mechanical analysis

The fatigue crack growth and stress intensity factor (K) are usually investigated in fracture analysis. Because of the two dimensional feature geometry and loading condition, Mode I and II are considered in the linear analysis of elastic fracture mechanics by using the finite element method. In addition,

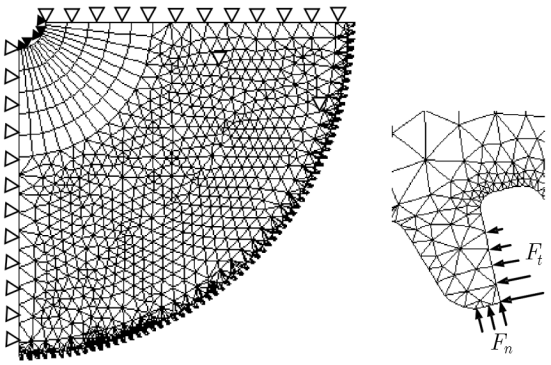

Fig. 4. Finite element model of the circular saw, its boundary conditions and forces applied to teeth

the node displacement method is considered to calculate the stress intensity factors. This method is appropriate for numerical solutions based on the finite element method, and is one of the most popular techniques used to calculate the stress intensity factors in numerical studies of fractures (Aslantaş and Taşgetiren, 2004). After obtaining finite element solutions for the cracked

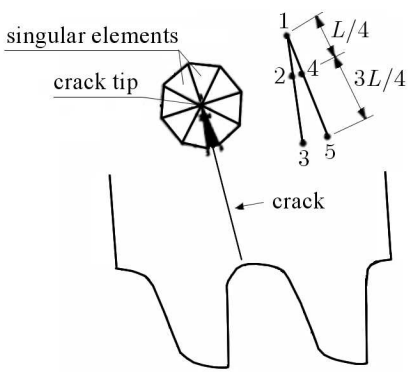

Fig. 5. Location of nodes used for calculation of the stress intensity factor

structure, the displacements of nodes 1-5 (Fig. 5) are determined. The stress intensity factors K_I and K_{II} for the opening and sliding modes are given by (Tan and Gao, 1990)

$$K_I = \frac{G}{\kappa+1}\sqrt{\frac{2\pi}{L}}[4(v_2 - v_4) + (v_5 - v_3)]$$
$$K_{II} = \frac{G}{\kappa+1}\sqrt{\frac{2\pi}{L}}[4(u_2 - u_4) + (u_5 - u_3)] \tag{3.1}$$

where G is the shear modulus and κ is defined for the plane stress condition as

$$\kappa = \frac{3-\nu}{1+\nu} \tag{3.2}$$

and L is the element length, ν is Poisson's ratio and u_i and ν_i $(i = 2, 3, 4, 5)$ are nodal displacements of the nodes in the x and y directions, respectively. In fracture mechanics, the critical stress intensity factor at the crack tip is used as the failure criterion under static loading. The critical value is called the fracture toughness and designeted by K_{IC}. The stress intensity factor increases with the increasing crack length. When the crack reaches a certain length, the stress intensity factor tends to fracture toughness and failure occurs. The fatigue crack propagation behaviour is expressed by the Erdogan-Paris equation (Ergun *et al.*, 2006)

$$\frac{da}{dN} = c(\Delta K)^m \tag{3.3}$$

where da is the increase of the crack length for dN cycles, ΔK is the range of the stress intensity factor, c and m are constants which depend on material properties. The material parameters having the microstructure given in Fig. 3 and mechanical properties given in Table 2 are given as in the literature, i.e. $c = 3.31 \cdot 10^{-17}$, $m = 4.16$ and $K_{IC} = 85\,\mathrm{MPa}\sqrt{\mathrm{m}}$ (Glodez *et al.*, 2002). The crack propagation of the opening mode is obtained from equation (3.3). For the mixed mode loading, the stress intensity factor range must be changed with an effective value. It is (Aslantaş and Taşgetiren, 2004)

$$\Delta K_{eff} = \sqrt[4]{\Delta K_I^4 + \Delta K_{II}^4} \tag{3.4}$$

The fatigue crack growth is assumed to occur either in the plane of the maximum shear stress intensity factor range or that of the maximum tensile stress intensity range (Aslantaş and Taşgetiren, 2004). The most widely accepted method for the prediction of propagation direction is the maximum principal stress theory. Depending on this theory, the crack propagates in the direction perpendicular to the maximum principal stress. The crack propagation direction is found from

$$\theta = 2\tan^{-1}\left[\frac{1}{4}\left(\frac{K_I}{K_{II}} \pm \sqrt{\left(\frac{K_I}{K_{II}}\right)^2 + 8}\right)\right] \tag{3.5}$$

4. Results and discussions

4.1. Stress analysis

The stress analysis is carried out under the given load condition in the plane stress state. While cutting forces vary with different factors, the critical region is the same for the circular saw. Figure 6 shows the first principal stress distribution of the model. The critical stress concentration takes place at the tooth root region during the cutting process because of cutting forces, and this concentration cause initiation of fatigue cracks. As can be seen, the maximum stress occurred is about 2/3 of the yield strength.

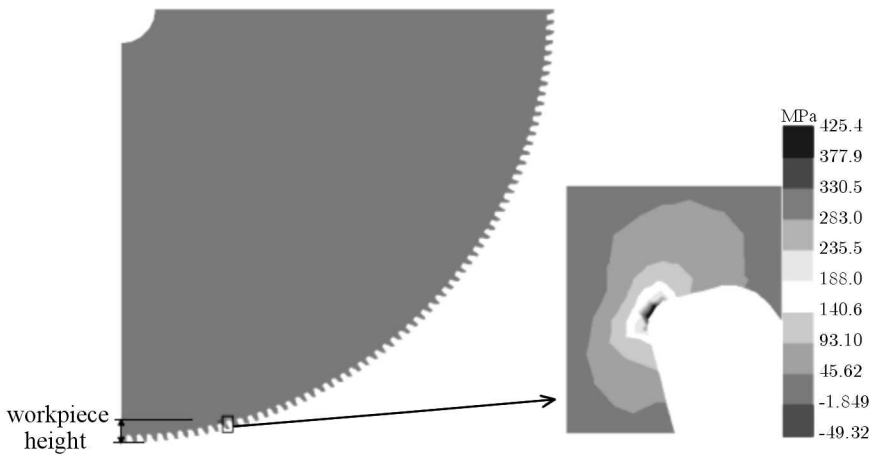

Fig. 6. Principal stress distribution in the circular saw during the cutting process for 2880 rpm and 10 mm in cut depth

4.2. Analysis of fractography

As mentioned above, the critical stress concentration in the circular saw occurs particularly at the tooth root region under variable forces. Loads which act in the tooth root region are tension forces, and they produce cracks at this region. Two different cracks close to each other occurred in the saw analysed in this study. Figure 1 shows the damaged area of the saw, and small and large cracks.

As can be seen, fatigue cracks initiate in the disk firstly and grow in the same direction toward to the center of the circular saw. Then, both cracks change their direction to the cutting side. Figure 7a shows a SEM photograph of the abrupt change of the direction for a large crack, and the fracture surface

of it is shown in Fig. 7b. Figures 8a and 8b also show SEM photographs of the starting points for the small and the large cracks, respectively.

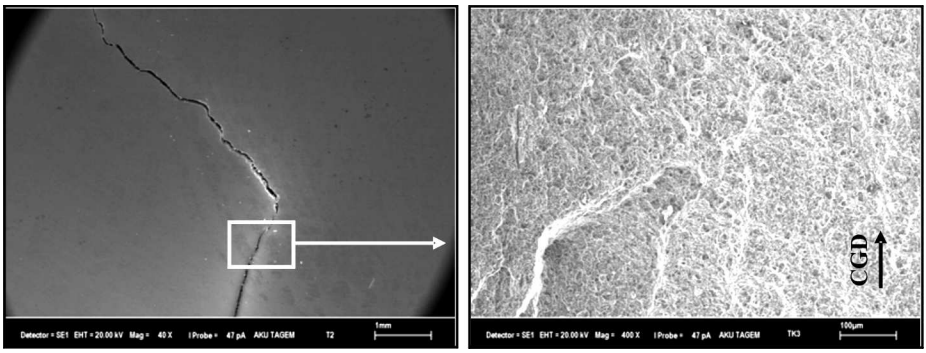

Fig. 7. (a) Change in the direction of the large crack growth, (b) fracture surface of the circular saw

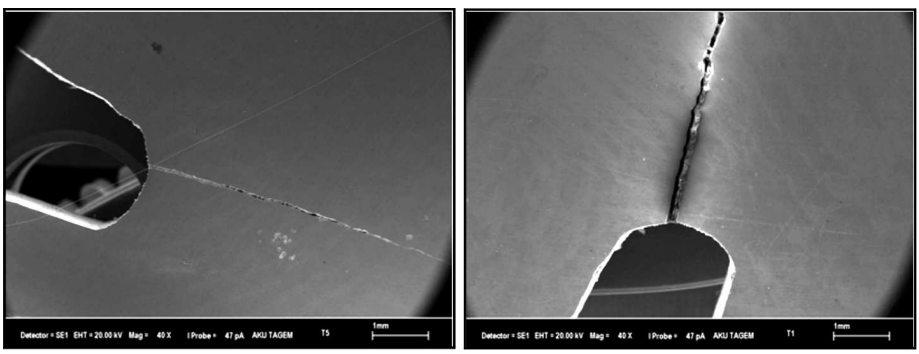

Fig. 8. SEM photographs of (a) small (b) large cracks

4.3. Calculation of the stress intensity factors

The stress intensity factors for a given crack and loading configuration are calculated by Eqs. (3.1). When a propagating crack is considered, the stress intensity factors and crack growth direction must be calculated for each increasing crack length. The sign of $K_I I$ is important for determining the crack growth direction. Paris and Erdoğan (1961), Erdoğan and Sih (1963) shown that a crack continues to advance in its own plane when it is subjected only to mode I. The presence of positive K_{II} at the crack tip means a clockwise turn of the direction, while a negative K_{II} means a counterclockwise turn. In

order to calculate the time elapsed for a certain crack length, the following procedures are practiced for each loading cycle:

- firstly, K_I and K_{II} are calculated for the initial crack length, and then ΔK is calculated using Eq. (3.4) for the crack configuration,
- secondly, da is determined by consideration of parameters c and m.

This is added to the original crack length to obtain the new crack condition by taking the effect of the crack front growing direction. The number of cycles is recorded and the procedure is repeated until the desired crack length is achieved. In the analysis, variations of K_I and K_{II} are shown in Figs. 9 and 10.

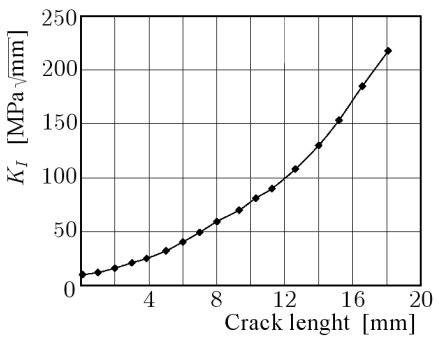

Fig. 9. Variation of K_I with length of the large crack

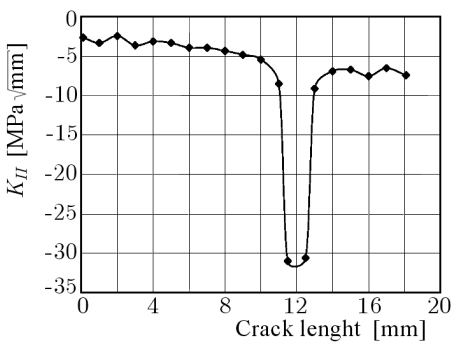

Fig. 10. Variation of K_{II} with length of the large crack

In the numerical analysis, the fatigue life of the circular saw is found from Eq. (3.3) as $1.02 \cdot 10^8$ cycles after the crack initiation. In addition, the fatigue life of the saw is found as $2.327 \cdot 10^8$ cycles before the crack initiation (Glodez *et al.*, 2002). If this life is compared to the life of the circular saw under working conditions, they are in good agreement. Finally, the total life of the saw is

approximately equal to $3.347 \cdot 10^8$ cycles. If the saw is used 2 or 3 hours daily to cut metals, its life will be 966 or 645 days, respectively. When they are compared to real applications, these results are reasonable.

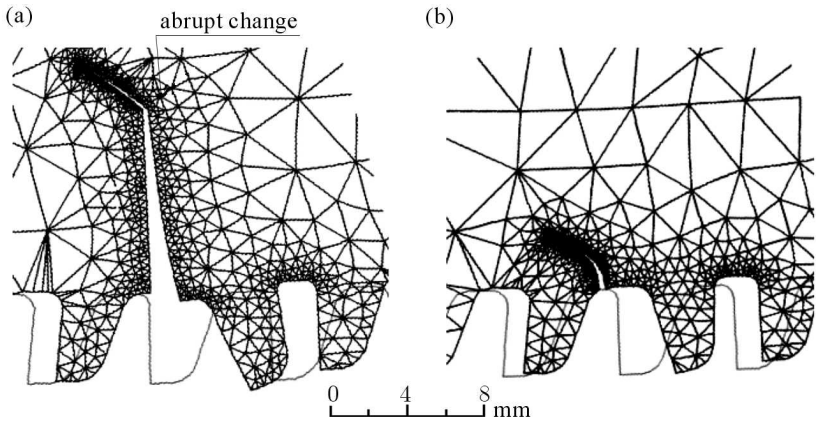

Fig. 11. Finite element model of (a) large crack (b) small crack

The finite element method results of the fracture analysis are shown in Fig. 11. The crack grows upward and then changes its direction to the cutting side in the numeric investigation as it occurred in the sample disc analysed in this study. Small and large cracks change their directions after the critical point and their lengths are different for each crack. The reason of it might be the initiation site of the crack, which is a subject of another study. In the numerical analysis, the crack also changes its direction to the same side. In addition, since the saw is investigated as a two-dimensional problem, lateral loads are disregarded. These loads are very small and do not affect the fatigue life.

5. Conclusion

Mechanical and micro-structural properties as well as chemical compositions are examined for a circular saw. In addition, fractographic, stress, and fracture analyses are carried out to determine the possible fracture reasons and the fatigue life of the circular saw. Cracks occurred at the tooth root region where the stress concentration is maximum during the cutting process and close to each other in the circular saw. Both cracks grow toward the center of the circular saw. In addition, the cracks shift their directions to the cutting side of

the saw after a point which is the critical condition for the saw. Experimental and numerical findings for fatigue crack propagations are in good agreement. The value of K_{II} is usually used to determine the crack direction. K_I is also determined in numerical analysis. As a result of the numerical fracture analysis, the fatigue life is estimated as $1.02 \cdot 10^8$ cycles after the crack initiation. The total life of the saw is approximately equal to $3.347 \cdot 10^8$ cycles. This result is reasonable for real applications. Finally, undesired shock forces during the cutting process might be effective for fracture in addition to the feed rate, revolution speed of the saw, types of material being sawed, depth of cut, and material defects in the circular saw.

Acknowledgements

The authors gratefully acknowledge the support of the Research Foundation of Afyon Kocatepe University in this study. This paper was also presented at the 8th International Fracture Conference, 7-9 November 2007, Istanbul, Turkey.

References

1. Akkurat M., 1996, *Talaş kaldırma metotları ve takım tezgahları (Chip removing methods and tool machines)*, Birsen publishing, Istanbul, Turkey
2. Andersson C., 2001, Bandsawing Part III: Stress analysis of saw tooth microgeometry, *International Journal of Machine Tools and Manufacture*, **41**, 255-263
3. Aslantaş K., Taşgetiren S., 2004, Modelling of spall formation in a plate made of austempered ductile iron having a subsurface-edge crack, *Computational Materials Science*, **29**, 29-36
4. ASM Specialty Handbook; Carbon and alloy steels, 1996, *ASM International*, p. 19
5. Bootroyd G., 1989, *Fundamentals of Metals Machining and Machine Tools*, Mcgraw Hill, United State of America, New York
6. Erdoğan F., Sih G.C., 1963, On the crack extension in plates under plane loading and transverse shear, *J. Basic Eng.*, **85**, 519-527
7. Ergun E., Aslantaş K., Taşgetiren S., Topçu M., 2006, Fracture analysis of resistance welded *L*-shaped and straight sheets, *Materials and Design*, **27**, 2-9
8. FRANC2D, User's Manual, Available in www.cfg.cornell.edu

9. Fukaura K., Yokoyama Y., Yokoi D., Tsujii N., Ono K., 2004, Fatigue of cold-work tool steels: effect of heat treatment and carbide morphology on fatigue crack formation, life, and fracture surface observation, *Metallurgical and Materials Transactions A*, **35(04A)**, 1289
10. Glodez S., Sraml M., Kramberger J., 2002, A computational model for determination of service life of gears, *International Journal of Fatigue*, **24**, 1013-1020
11. Heat Treaters Guide: Practices and procedures for irons and steels, 1995, *ASM International*, 313-340 and 889
12. Nordström J., Bergström J., 2001, Wear testing of saw teeth in timber cutting, *Wear*, **250**, 19-27
13. Paris P.C., Erdoğan F., 1961, A critical analysis of crack propagation laws, *J. Basic Eng.*, **85**, 528-534
14. Tan C.L., Gao Y.L., 1990, Treatment of bimaterial interface crack problems using the boundary element method, *Eng. Fract. Mechanics*, **36**, 6, 919-932
15. Topbas M.A., 1998, *Çelik el kitabı ve ısıl İşlem (Steel handbook and heat treatment)*, October Press, Istanbul [in Turkish]
16. Yesildal R., Sen S., Kaymaz I., 2003, Fatigue behaviour of X40CrMoV 51 at high temperatures, *Journal of Materials Engineering and Performance*, **12**, 2, p. 215

Inicjacja i wzrost pęknięcia w pile tarczowej wykonanej ze stali narzędziowej

Streszczenie

Przedmiotem badań jest wytrzymałość zmęczeniowa piły tarczowej wykonanej ze stali narzędziowej i przeznaczonej do pracy w przemyśle metalurgicznym, w szczególności do cięcia prętów i rur. Z powodu niewielkiego promienia zaokrąglenia podstawy zęba tarczy, piły narażone są na pęknięcia właśnie w tym obszarze. Na rozwój procesu pękania mają wpływ obciążenia promieniowe i styczne zęba. Tu występuje największa koncentracja naprężeń przy znacznych prędkościach obrotowych tarczy i dużego tempa posuwu. Do przeanalizowania procesu zmęczenia piły użyto próbek wypreparowanych ze zniszczonego narzędzia i poddano je licznym testom mechanicznym. Równolegle przeprowadzono symulacje teoretyczne za pomocą Metody Elementów Skończonych. Przyczyny i wyniki ilościowe dotyczące zniszczenia zmęczeniowego wyznaczono na podstawie obydwu metod badawczych i następnie je porównano.

Manuscript received November 8, 2007; accepted for print February 15, 2008